Methods for investigation of electrical contact resistance in a metal film–semiconductor structure

© M.Yu. Shtern[1], I.S. Karavaev[2], M.S. Rogachev[1,¶], Yu.I. Shtern[1], B.R. Mustafoev[1], E.P. Korchagin[1], A.O. Kozlov[1]

[1] National Research University of Electronic Technology, 124498 Moscow, Zelenograd, Russia
[2] JSC „Chepetsky Mechanical Plant", 427622 Glazov, Russia

¶ E-mail: m.s.rogachev88@gmail.com

Received September 19, 2021
Revised September 24, 2021
Accepted September 24, 2021

The electrical contact resistance significantly affects the efficiency of thermoelements. In the case of high doped thermoelectric materials, the tunneling mechanism of conductivity prevails at metal-semiconductor interface, which makes it possible to obtain a contact resistance of less than $10^{-8}\,\Omega\cdot m^2$. Low resistance values significantly complicate its experimental determination. Work present three techniques and a measuring stand for the investigation of contact resistance. The techniques are based on the measurement of the total electrical resistance, which consists of transient contact resistance and the resistance of the thermoelectric material with its subsequent exclusion. The developed techniques differ in the arrangement of the investigated contacts on the samples, in the methods of measurement and processing of the obtained results, and make it possible to determine the specific contact resistance of the order of $10^{-10}\,\Omega\cdot m^2$.

Keywords: thermoelements, film contacts, contact resistance, measurement techniques.

DOI: 10.21883/SC.2022.01.53115.24

1. Introduction

One of the main characteristics of film contacts formation in semiconductor structures is contact resistivity that significantly affects their efficiency. In thermoelements this parameter value is especially critical since thermoelectric materials (TEM), of which the thermoelements are made, have high electrical conductivity. Charge carriers concentration in TEM is usually $10^{19}-10^{20}\,cm^{-3}$. In this case the specific weight of contact resistance can be crucial in thermoelement structure and can significantly impact its thermal and electrophysical parameters. Therefore, the ohmic contacts are essential for thermoelements technology. Ohmic contacts are metal–semiconductor contacts, which resistance is negligible compared to volume resistance of semiconductor at any current direction. According to the author of study [1], the ohmic contact should have resistivity of $< 10^{-7}\,\Omega\cdot m^2$. In case of contact for TEM this value should be not more than $10^{-8}\,\Omega\cdot m^2$ [2–6]. Significant impact of contacts resistance on thermoelectric devices efficiency is specified by several authors [2–9]. According to author of study [10], in case of increase of contact resistance in thermoelements, operating through Peltier effect, to 1% of thermoelement resistance, the temperature difference (its main parameter) is reduced to 30% of maximum value. In study [11] it was observed that the maximum value of efficiency in generator thermoelements can be achieved at contacts resistivity on a level of $10^{-10}\,\Omega\cdot m^2$.

The required condition of Ohmic contact presence at metal–semiconductor interface is a low value of Schottky barrier. Two conductivity mechanisms are connected with Schottky barrier: thermoelectron emission and tunneling [12–14]. Two empirical methods of contacts producing are connected with these mechanisms. The first one consists in selection of metal (as per work function), that creates low Schottky barrier together with semiconductor. Ohmic contacts can be made using metals with work function that is less than for semiconductor of *n*-type and more than for semiconductor of *p*-type. However, there are very small number of metal–semiconductor combinations that satisfy this condition. At the same time it was experimentally revealed for the majority of semiconductors, that energy barrier does not depend on metal work function, but is defined with surface states density [1,12]. Therefore, the commonly used method of ohmic contacts producing is a heavy doping of semiconductor for the contact, sufficient enough to provide charge carriers tunneling through the barrier. The prevailing tunneling current component exponentially depends on free charge carriers concentration [12]. At concentration of $\sim 10^{19}\,cm^{-3}$ the contact resistance is mainly defined with tunneling processes, that is characteristic for TEM.

Low values of contact resistance in semiconductor — metal contact structure significantly complicate its experimental determination. The method of contact resistance measurement similar to well-known method of TLM (Transmission line method) [8,15–18] is proposed in this study.

Total electrical resistance, consisting of contact resistance and substrate resistance, is measured with its following exclusion. Our case is based on TEM samples, on which the metal contacts are formed using ion-plasma deposition.

According to studies performed under this work, the implementation methods of the specified method for measuring the low contact resistance (measurement techniques) are important for stable data acquisition with minimum measurement errors. The techniques proposed in this study have differences in terms of location of the studied contacts on TEM samples, methods of measurements and the observed results processing.

Thus, the purpose of this study is development and research of experimental techniques of contact resistance of metal films, formed on semiconductor materials, TEM in this case, as well as comparative analysis of data observed using these techniques for measurements optimization.

2. Experimental part

2.1. Samples preparation

During development of techniques of contact resistance measurement the nickel contacts, formed with ion-plasma deposition on samples of $Bi_2Te_{2.8}Se_{0.2}$, alloyed with 0.14 weight% $CdCl_2$, made using zone melting, were used.

Condition of TEM surface significantly impacts the contacts characteristics [17,19–22]. Before application of thin films of Ni the mechanical processing of TEM samples surface to roughness of 150 nm was performed with the following cleaning, which methods are presented in [20]. Samples surface roughness and film thickness were measured using profile meter KLA-Tencor P-7.

Before loading into deposition system chamber the samples were cleaned with isopropyl alcohol with the following drying with nitrogen. Contacts formation was performed using high-vacuum deposition system Angstrom EvoVac 34. Vacuum thermal annealing of TEM samples was performed directly in the chamber with initial pressure of $7 \cdot 10^{-8}$ Torr and temperature of 200°C. After annealing the samples surface cleaning was performed with argon ions bombardment for 30 s. During vacuum thermal annealing using quadrupole SRS RGA 200, that is a part of the deposition system, the quality of the samples surface finishing was controlled.

Ion-plasma deposition of nickel contacts with thickness of 300 nm was performed after ion cleaning and operating pressure achieving in the chamber. The following deposition modes were used: chamber pressure — $7 \cdot 10^{-8}$ Torr, deposition rate — 2 Å/s, gas pressure (Ar) — $2 \cdot 10^{-3}$, temperature — 200°C.

Contact areas forming on side surfaces of TEM samples was performed using masks made of aluminum alloy foil with thickness of 0.1 mm, in which the windows with diameter of 1.5 mm were made using laser machine BetaMARK 2000. Distance between contacts was defined with accuracy of 50 μm.

TEM samples of certain shape and location of examined contacts were prepared for each technique. Samples № 1 were made as cylinders with length of 30 mm and diameter of 10 mm. Mechanical processing of samples side surface along crystal growth direction was performed for contacts producing. Contact areas of Ni with diameter of 1.5 mm were formed through deposition on the resulting plane every 5.0 mm, and to these areas the current and potential contact wires were soldered.

Samples № 2 were made as discs with diameter of 20 mm and thickness of 2 mm. These samples cutting was performed in direction, perpendicular to crystal growth. After that the mechanical processing of samples surface was performed, when on every 5 mm of the surface the nickel contact areas with diameter of 1.5 mm were formed. Commutation of current and potential wires to contact areas was performed with soldering.

Samples № 3 were made similar to samples № 1, but on opposite ends of TEM samples the contact areas of Ni with thickness of 300 nm were additionally formed with ion-plasma deposition. Plates of Ni with thickness of 1 mm were soldered to contact areas at the ends. Commutation potential wires for voltage drop measurement were soldered to contact areas formed on sample side surface.

Samples № 4 were made as cylinders with length of 20 mm and diameter of 10 mm. Samples side surface and ends were mechanically processed to roughness of 150 nm. Contact areas of Ni, to which the nickel plates with thickness of 1 mm were soldered, were formed at opposite ends of sample using ion-plasma deposition.

2.2. Measurement techniques

For implementation of contact resistance measurement techniques the stand was developed, including: measuring cell, equipped with micrometric measuring indicators and digital microscope with visualizer; multimeter Keithley 2001 (M); high-accuracy electronic thermometer TEN-4; programmable power supply Motech LPS-305 (A) with integrated amperemeter and voltmeter; high-accuracy resistance box Time Electronics 1067 (RB). Measured data from multimeter, thermometer and microscope come to computer, that is a part of stand structure.

At low resistance values, which include the examined contact resistance of contact — TEM structure, short circuit is almost happened in the measuring circuit for power source. In this case the majority of sources can not stabilize the specified current with acceptable accuracy. Therefore, the resistance box is sequentially included in the measuring circuit to the sample. By means of regulation of parameters of power source and resistance box in the circuit the required current value was set, that was stabilized with error, not exceeding 0.1%.

During measurements the temperature profile was controlled at TEM sample using two thin-film platinum thermoresistors Pt-1000, installed in current probes. Thermoresistors were connected to thermometer TEN-4 with

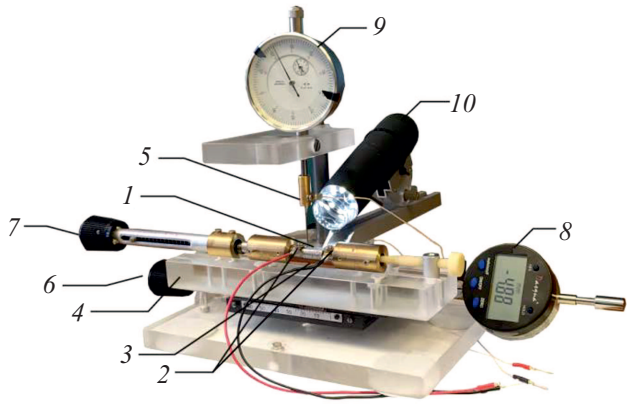

Figure 1. Measuring cell for contact resistance determination.

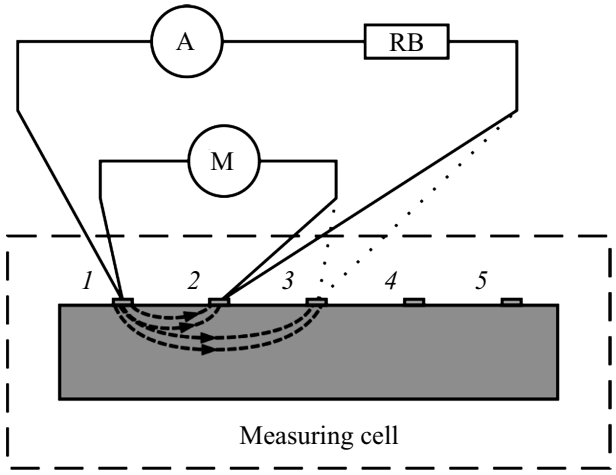

Figure 2. Schemes of samples № 1 and № 2 and contact resistance measurements as per the first technique.

measurement error of 0.05°C. Voltage measurement error did not exceed 0.2% considering multimeter sensitivity of (10^{-7} V). It should be noted that at measurement of voltage drop on the examined structures the four-wire scheme was used, allowing to remove errors, defined by the lead resistance. Current was passed through the sample in two opposite directions. Direct current direction change is required to remove thermoelectric effects influence on measurement results.

Measuring cell design is presented in Fig. 1. The examined TEM sample (*1*) was placed between current probes (*2*), in copper mountings (*3*), through mica with thickness of 20 μm. This allows to minimize the temperature gradient on the sample during measurements. Current probes contact area should not be less than cross section of the examined samples. Copper mounting with the sample was fixed on a base (*4*), which movement relating to measuring probe (*5*) was regulated using precision mechanism (*6*). Probe scanning step was regulated such way. Measuring probe is made of steel needle with gold cover. Force of load on TEM sample, located between current probes, was defined using the device (*7*). Micrometric indicator was used to control the movement of the base with the sample and, consequently, measuring probe scanning step (*8*). Probe position was defined with error of 10 μm. Force of clamping the measuring probe to the examined sample was controlled using calibrated micrometric measuring indicator (*9*). Digital microscope (*10*), connected with PC, was used for measurement process visualization.

The first measurement technique. The first technique for contact resistance measurement the samples № 1 and № 2 were used. Scheme of contact resistance measurement is presented in Fig. 2. Numbers of contact areas on the sample side surface are designated with digits. As was shown above, the four-wire scheme was used during measurements of voltage drop on the examined structures. During measurement of contact resistance the examined sample was put into the measuring cell and fixed between current probes. For the first technique these probes were used only for fixing the examined sample in the cell and temperature measurement in it. Current was supplied to the sample using current wires soldered to the contact areas. Current with value of 100 mA from the power source (A) was supplied between the contact area № 1 and contact

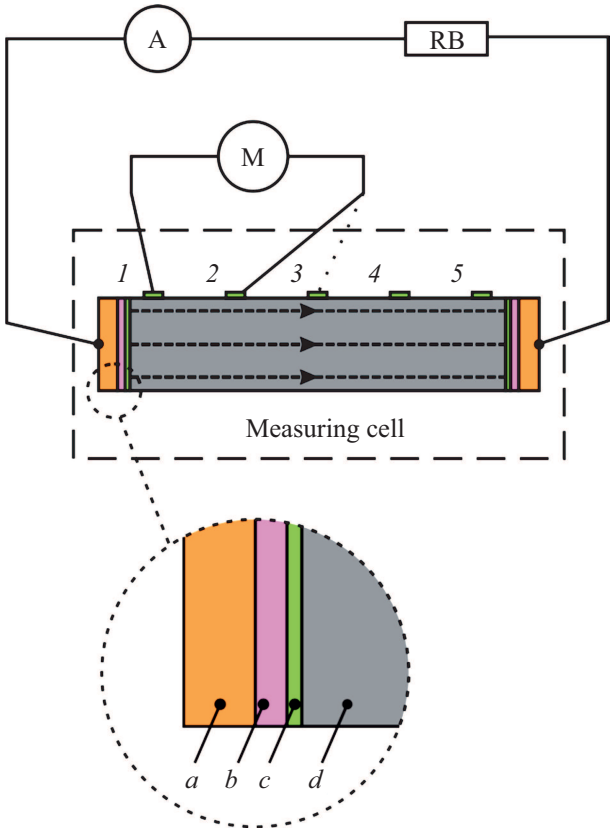

Figure 3. Schemes of sample № 3 and measurements of contact resistance as per the second technique. *a* is the Ni-plate, *b* is the solder, *c* is the nickel contact area, *d* is the TEM sample.

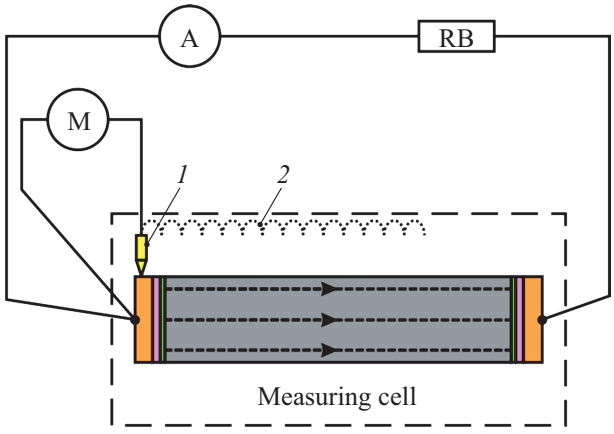

Figure 4. Scheme of contact resistance measurement as per the third technique. *1* is the measuring probe, *2* is the measuring probe movement pattern.

areas № 2–5 sequentially. Voltage drop was measured with multimeter (M) using potential wires. Measurements were performed with the opposite current directions.

The second measurement technique. Schemes of contact resistance measurement as per the second technique and contacts location on the sample are presented in Fig. 3.

During measurement of contact resistance as per the second technique the TEM sample № 3 was used and was put into the measuring cell between the current probes. Using the probes connected to power source the current of 100 mA was passed through the sample. Voltage drop was defined using potential wires between the first contact area and the rest contact areas, formed on the side surface, sequentially. Measurements were performed with the opposite current directions.

The third measurement technique. Sample № 4 was used for studying the contact resistance as per the third technique. Scheme of contact resistance measurement is presented in Fig. 4. The sample is put into the measuring cell between the current probes. Sample movement and, consequently, measuring probe scanning along the sample side surface was performed with a step from 50 to 500 μm and controlled using micrometer indicator. Measurement was performed with the measuring probe scanning over the whole length of TEM sample from one nickel plate on the sample end to another. After measuring probe installation the current of 300 mA was passed through the sample from the power source using the current probes. Two measurements of voltage drop between the end nickel plate and the measuring probe with the opposite current directions were performed in each point on sample surface as per the scanning step.

3. Study results and discussion

At first the structure resistance was calculated for determination of the contact resistance of the examined structures as per the first and second techniques using the formula

$$R = U/I, \tag{1}$$

where U is the voltage drop, I is the current.

During measurements the current was passed in two directions, while voltage drop on the structure was defined using the formula

$$U = (|U_1| + |U_2|)/2, \tag{2}$$

where U_1 and U_2 are the voltage drops at current passing in two opposite directions.

Contact resistance was calculated the following way. Resistances were measured, for instance, R_{str12} and R_{str13}. Resistance R_{str12} between contact areas 1 and 2 (Figs. 2 and 3) includes resistance of contacts 1 and 2 (R_c), as well as TEM resistance at the area between these contacts (R_{M12}):

$$R_{str12} = 2R_c + R_{M12}. \tag{3}$$

Therefore, R_{str13} will be equal to:

$$R_{str13} = 2R_c + R_{M13}. \tag{4}$$

Ratio of R_{M12} and R_{M13} is defined by the distances between the contact areas 1, 2 and 1, 3. Since contacts are formed on the same distance,

$$R_{M13} = 2R_{M12}. \tag{5}$$

Then the contact resistance can be calculated using the formula

$$R_c = (2R_{str12} - R_{str13})/2. \tag{6}$$

Contact resistivity considering contact area (S_c) was defined the following way:

$$\rho_c = R_c S_c. \tag{7}$$

TEM, made by direct crystallization, have an anisotropy of properties, including electrical conductivity. Therefore, the measurement of contact resistance at current passing along (sample № 1) and across (sample № 2) TEM crystal growth direction is of interest for validation of the observed results. Best case scenario, the measured contact resistances, observed on both samples, cut from TEM crystal ingots along and across its growth, should have the same values.

The measurement results, observed at implementation of the first technique (samples № 1 and № 2) and the second technique (sample № 3), are presented in the table.

Analyzing the observed data it should be noted that electrical resistance of structure (R_{str}) of samples № 1 and № 2 is different. This is defined by anisotropy of values of TEM electrical conductivity. Particularly, TEM electrical conductivity along crystal growth axis is higher than in perpendicular direction. This effect has no influence on contact resistance. Therefore, the observed values of R_c and ρ_c on samples № 1 and № 2 differ not more than it is defined by the measurements error.

Results of contact resistance study

Sample №	I, mA	U_{12}, μV	U_{13}, μV	R_{str12}, mOhm	R_{str13}, mOhm	R_c, mOhm	ρ_c, Ohm · m^2
1	100	644	1141	6.44	11.41	0.74	$1.3 \cdot 10^{-9}$
2	100	820	1502	8.20	15.02	0.69	$1.2 \cdot 10^{-9}$
3	100	476	641	1.59	2.14	0.51	$0.9 \cdot 10^{-9}$

Values of contact resistance, defined as per the first and second techniques, are different, that is probably caused with current lines distribution during measurements. In this regard the second technique is preferable, since current lines are evenly distributed in it. Current distribution influence on accuracy of electrophysical measurements is also mentioned by the authors [23,24].

Sample № 4 was used for studying the contact resistance as per the third technique. Nickel plate in the end contact of this sample performed two functions. The first one is an area for measuring probe installation (it is not possible to install the probe on a film with thickness of 300 nm). The second one (as for sample № 3) is the even distribution of current lines along sample cross section at current passing through it.

During probe scanning over the surface of the sample the voltage drop between the nickel plate and measuring probe was measured. Then, the existing resistance was calculated using the formula (1). During study using this technique the current, passed through the sample, was increased to 300 mA. This is necessary to compensate the error, appearing due to decrease of distance between the measurement points, resulting in significant reduction of the measured voltage.

During probe movement over the sample the scanning step changed. In the area of measured contact the step was 50 μm, that relates to necessity of more accurate determination of its position. Such accuracy is not required at the probe scanning over thermoelectric material. Therefore, for measurements promptness the step was increased to 500 μm.

Resistance variation during probe movement over the sample was schematically shown in Fig. 5. Value of contacts resistance was defined by means of increase of the measured resistance at probe transition from nickel plate to TEM on one end of the sample or from TEM to nickel plate on another end of the sample. Contacts resistance was defined the following way:

$$R_{c1} = R_1 - R_{p1}, \tag{8}$$

$$R_{c2} = R_{p2} - R_2, \tag{9}$$

where R_{p1} and R_{p2} are measured resistances at nickel plates. R_1 and R_2 are measured resistances in the beginning and end of TEM sample, respectively (Fig. 5).

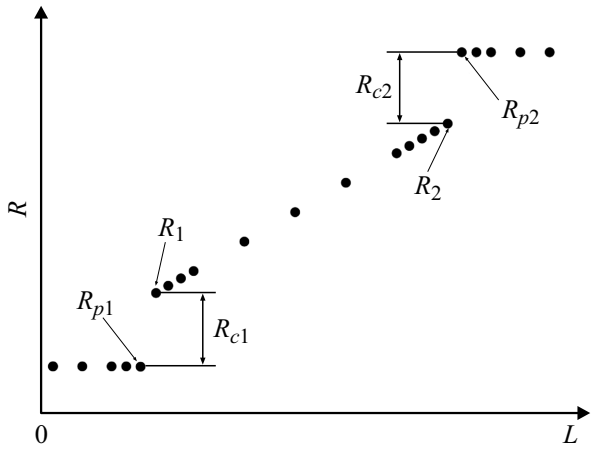

Figure 5. Scheme of electrical resistance variation depending on measuring probe position on TEM sample.

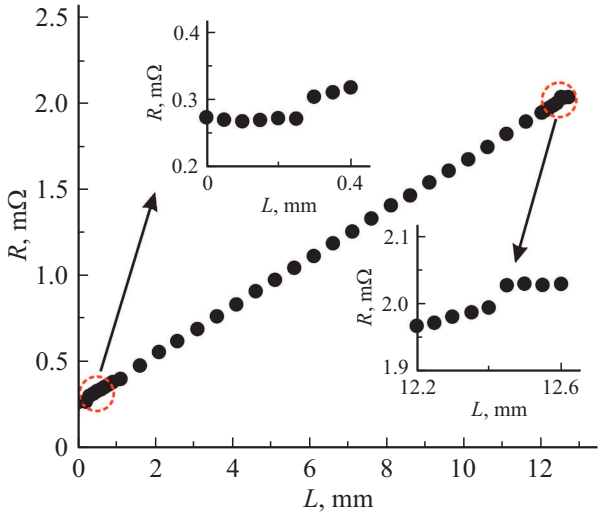

Figure 6. Dependence of electrical resistance on sample № 4 on measuring probe position.

It should be noted that at the same time the TEM resistance presents in contacts resistance values. This is defined by the fact that the minimum step of the measuring probe movement (50 μm) is significantly higher than thickness of Ni deposited layer (300 nm). But this increase of contact resistance does not significantly impact the measurement results, since it is defined by the small thickness of TEM layer and its high electrical conductivity. Also, TEM contribution into the contact resistance can be calculated.

During measurements two values of contact resistance on the opposite ends of the sample were defined. Average value was calculated the following way:

$$R_{c.av} = (R_{c1} + R_{c2})/2. \tag{10}$$

Contact resistivity was defined using the formula (7). Experimental data from the sample № 4 contact resistance study are presented in Fig. 6.

During movement of the measuring probe on the first section the resistance has small variations and is defined by the nickel plate resistance (Fig. 6). At the measuring probe transition from the nickel plate to TEM sample the sharp increase of resistance is observed. Then, at probe scanning over the sample, the TEM-defined resistance increases linearly with distance. In the end of the sample, at probe transition to the nickel plate, the second significant increase of resistance is observed. Sharp change of resistance in the beginning and end of the sample is defined by contact resistance. Contact resistivity, determined using the third technique, was $2.2 \cdot 10^{-9}\,\mathrm{Ohm} \cdot \mathrm{m}^2$.

The proposed techniques can be used for studies during development of contact systems technology for semiconductor materials, equally including TEM. The technique selection can be made considering process capabilities of researchers at contacts producing.

According to studies, the contact resistivity of $\sim 10^{-10}\,\mathrm{Ohm} \cdot \mathrm{m}^2$ can be defined with acceptable error, indicating the high sensitivity of the techniques. For each technique the measurement errors were defined considering samples size and selected research modes. For the first two techniques the error is at the level of $3 \cdot 10^{-10}$ and $1 \cdot 10^{-10}\,\mathrm{Ohm} \cdot \mathrm{m}^2$, respectively. For the third technique the error was $5 \cdot 10^{-10}\,\mathrm{Ohm} \cdot \mathrm{m}^2$. The largest part of the third technique error was related to determination of the measuring probe position and it can be reduced, as was shown above, using the calculation.

The observed results are in good agreement with literature data for high-quality thin film contacts, formed with vacuum deposition [16,19,25–27]. It should also be noted that low values of contact resistance indicate the quality of production technology of film contacts for TEM, presented in this study.

It should be noted that the third measurement technique can be used for determination of electrical conductivity of thermoelectric materials.

4. Conclusion

Three techniques and the measuring stand are developed for studying the contact resistance in film metal contact — semiconductor structure. Experimental approbation of the techniques was performed at metal film — thermoelectric material structures, in which the contact resistivity is $\sim 10^{-9}\,\mathrm{Ohm} \cdot \mathrm{m}^2$. The techniques have differences in terms of location of the studied contacts on TEM samples, methods of measurements and the observed results processing.

High sensitivity of contact resistance determination on the level of $10^{-10}\,\mathrm{Ohm} \cdot \mathrm{m}^2$ was observed. Measurement errors were defined for each technique and they do not exceed $5 \cdot 10^{-10}\,\mathrm{Ohm} \cdot \mathrm{m}^2$. The proposed techniques can be used for studies during development of contacts technology for semiconductor materials, including contacts in thermoelements. Selection of one of the techniques can be made considering process capabilities of researchers at contacts producing.

Funding

This study was financially supported by the Russian Science Foundation (project No. 20-19-00494).

Conflict of interest

The authors declare that they have no conflict of interest.

References

[1] E.H. Rhoderick, R.H. Williams. *Metal-Semiconductor Contacts* (Oxford, University Press, 1988).
[2] R.P. Gupta, K. Xiong, J.B. White, K. Cho, H.N. Alshareef, B.E. Gnade. J. Electrochem. Soc., **157** (6), H666 (2010).
[3] A. Ferrario, S. Battiston, S. Boldrini, T. Sakamoto, E. Miorin, A. Famengo, A. Miozzo, S. Fiameni, T. Iida, M. Fabrizio. Materials Today: Proceedings, **2** (2), 573 (2015).
[4] M. Shtern, M. Rogachev, Y. Shtern, D. Gromov, A. Kozlov, I. Karavaev. J. Alloys Compd., **852**, 156889 (2021).
[5] G. Joshi, D. Mitchell, J. Ruedin, K. Hoover, R. Guzman, M. McAleer, L. Wood, S. Savoy. J. Mater. Chem. C, **7** (3), 479 (2019).
[6] W. Liu, H. Wang, L. Wang, X. Wang, G. Joshi, G. Chen, Z. Ren. J. Mater. Chem. A, **1** (42), 13093 (2013).
[7] T. Sakamoto, Y. Taguchi, T. Kutsuwa, K. Ichimi, S. Kasatani, M. Inada. J. Electron. Mater., **45** (3), 1321 (2016).
[8] Y. Thimont, Q. Lognone, C. Goupil, F. Gascoin, E. Guilmeau. J. Electron. Mater., **43** (6), 2023 (2014).
[9] K. Xiong, W. Wang, H.N. Alshareef, R.P. Gupta, J.B. White, B.E. Gnade, K. Cho. J. Phys. D: Appl. Phys., **43** (11), 115303 (2010).
[10] W. Hanlein. Kaltetechnik, **2**, 137 (1960).
[11] W. Liu, Q. Jie, H.S. Kim, Z. Ren. Acta Mater., **87**, 357 (2015).
[12] S.M. Sze, K.K. Ng. *Physics of Semiconductor Devices* (N.Y., Wiley, 2007).
[13] K.K. Ng, R. Liu. IEEE Trans. Electron Dev., **37**, 1535 (1990).
[14] T.V. Blank, Yu.A. Gol'dberg. FTP, **41** (11), 1281 (2007) (in Russian).
[15] V. Kessler, M. Dehnen, R. Chavez, M. Engenhorst, J. Stoetzel, N. Petermann, K. Hesse, T. Huelser, M. Spree, C. Stiewe, P. Ziolkowski, G. Schierning, R. Schmechel. J. Electron. Mater., **43** (5), 1389 (2014).
[16] D. Qin, W. Zhu, F. Hai, C. Wang, J. Cui, Y. Deng. Adv. Mater. Interfaces, **6** (20), 1900682 (2019).
[17] X. Zhu, L. Cao, W. Zhu, Y. Deng. Adv. Mater. Interfaces, **5** (23), 1801279 (2018).
[18] C.C. Yu, H.-j. Wu, M.T. Agne, I.T. Witting, P.-Y. Deng, G.J. Snyder, J.P. Chu. APL Mater., **7** (1), 013001 (2019).
[19] P.A. Sharma, M. Brumbach, D.P. Adams, J.F. Ihlefeld, A.L. Lima-Sharma, S. Chou, J.D. Sugar, P. Lu, J.R. Michael, D. Ingersoll. AIP Adv., **9** (1), 015125 (2019).
[20] M.Yu. Shtern, I.S. Karavaev, Y.I. Shtern, A.O. Kozlov, M.S. Rogachev. Semiconductors, **53** (13), 1848 (2019).
[21] E.K. Belonogov, V.A. Dybov, A.V. Kostyuchenko, S.B. Kushchev, D.V. Serikov, S.A. Soldatenko. Poverkhnost'. Rentgenovskie, sinkhrotronnye i nejtronnye issledovaniya, **5**, 17 (2019) (in Russian).

[22] D. Zillmann, D. Metz, B. Matheis, A. Dietzel, A. Waag, E. Peiner. J. Electron. Mater., **48** (9), 5363 (2019).
[23] A.T. Burkov, A.I. Fedotov, A.A. Kas'yanov, R.I. Panteleev, T. Nakama. Nauch.-tekhn. vestn. informatsionnykh tekhnologij, mekhaniki i optiki, **15** (2), 173 (2015) (in Russian).
[24] V.I. Smirnov, F.Yu. Matta. *Teoriya konstruktsij kontaktov v elektronnoj apparature* (M., Sov. radio, 1974) (in Russian).
[25] R.P. Gupta, J.B. White, O.D. Iyore, U. Chakrabarti, H.N. Alshareef, B.E. Gnade. Electrochem. Solid-State Lett., **12** (8), H302 (2009).
[26] P.J. Taylor, J.R. Maddux, G. Meissner, R. Venkatasubramanian, G. Bulman, J. Pierce, R. Gupta, J. Bierschenk, C. Caylor, J. D'Angelo. Appl. Phys. Lett., **103** (4), 043902 (2013).
[27] S.-P. Feng, Y.-H. Chang, J. Yang, B. Poudel, B. Yu, Z. Ren, G. Chen. Phys. Chem. Chem. Phys., **15** (18), 6757 (2013).